Microscopic Structural Features and Properties of Single Fibers from Different Morphological Parts of the Windmill Palm

Changjie Chen,[a,b] Guangxiang Sun,[a,b] Guicui Chen,[a,b,c] Xin Li,[a,b] and Guohe Wang [a,b]*

The chemical, morphological, physical, and thermal properties of raw materials and single fibers extracted from different morphological parts of windmill palm were examined and comprehensively characterized after an alkali treatment. Leaf sheathes (LS) with the highest cellulose content (52.26%) achieved the most efficient extraction of fibers. Single fibers extracted from the vascular bundles of the windmill palm raw material had a slender shape with a tapering and sealing terminus, with each single fiber possessing a lumen in its cross-section. These windmill palm fibers displayed similar chemical compositions, but they exhibited significant differences in morphological parameters. Leaf blade fibers (LBFs) had the longest length (1240 μm ± 470 μm) and highest aspect ratio (121.39), which presented excellent potential as a reinforced fiber. After the alkali treatment, almost all of the hemicelluloses and lignin were removed, which resulted in increased crystallinity of extracted fibers. Thermogravimetric analysis confirmed LS stability up to 319 °C, which was higher than that of other materials from windmill palm.

Keywords: Windmill palm; Morphological parts; Single fiber; Chemical composition; Morphological characteristics

Contact information: a: College of Textile and Clothing Engineering, Soochow University, Suzhou, 215006, P.R. China; b: Nantong Textile & Silk Industrial Technology Research Institute, Nantong, 226108, P.R. China; c: Jiangsu Research and Development Center of the Ecological Textile Engineering and Technology, Yancheng Institute of Industry Technology, Yancheng 224005, P.R. China;
** Corresponding author: wangguohe@suda.edu.cn*

INTRODUCTION

Trachycarpus fortunei, commonly known as the windmill palm tree, is a forest species of the Palmae family. In China, windmill palm trees occupy approximately 5,000,000 hectares of cultivated area. Residual agricultural materials are usually left in the soil and present a disposal problem (Sahari *et al.* 2012). Now in China most of the abundant, inexpensive, and readily available windmill palm leaf blades (LB), petioles (P) and fruit bunch (FB) are treated as waste. In practice this biomass is burned in field or as fuel, which creates environmental pollution problems. Leaf sheaths (LS) are used to make rope and other products with low additional value and low efficiency. The development of new applications for these agricultural residues could create a valuable economic opportunity for windmill palm producers and for regional economies.

Various studies related to the lignocellulosic fibers have been performed previously, including oil palm empty fruit bunch (EFB) (Sreekala *et al*. 2002; Yunos *et al*. 2014), kapok (Xiang *et al.* 2013), tea tree (Jammy *et al.* 2015), bamboo (Liu *et al*. 2011; Yang *et al*. 2015), sugar palm tree (Ishak *et al*. 2013), and many more, including banana, sugarcane bagasse, and sponge gourd fiber (Guimarães *et al*. 2009). Although

several studies have been performed on the structure and mechanical properties of windmill palm fiber from leaf sheaths (Zhai *et al.* 2012; Zhang *et al*. 2015), the general chemical composition, structure, and properties of all morphological parts of the windmill palm have not yet been assessed. However, this knowledge is crucial for exploring the potential additional applications for the processing of windmill palm material (Oliveira *et al.* 2007).

Alkaline treatment was used as a tool to facilitate lignocellulose fiber extraction (Khalil *et al.* 2012; Khalil *et al.* 2016; Paridah *et al.* 2016). Sodium hydroxide in combination with hydrogen peroxide is the most common way to separate cellulose fibers from wood and non-wood biomasses by completely eliminating amorphous hemicellulose and lignin content (Wang *et al.* 2011). This paper presents an investigation of the chemical composition, morphological structure, X-ray diffraction, and thermal behavior aspects of four different types of lignocellulosic fibers isolated by alkali treatment from the windmill palm tree. The windmill palm tree was fractionated into four morphological parts: P, LB, LS, and FB. The main objective of this research was to gain a better understanding of the structure and properties of different morphological parts of the windmill palm plant and to promote the better utilization of these materials.

EXPERIMENTAL

Materials

The windmill palm morphological parts P, LB, LS, and FB (Fig. 1) that were used in this study were obtained from windmill palm trees in the Suzhou Jiangsu province, China.

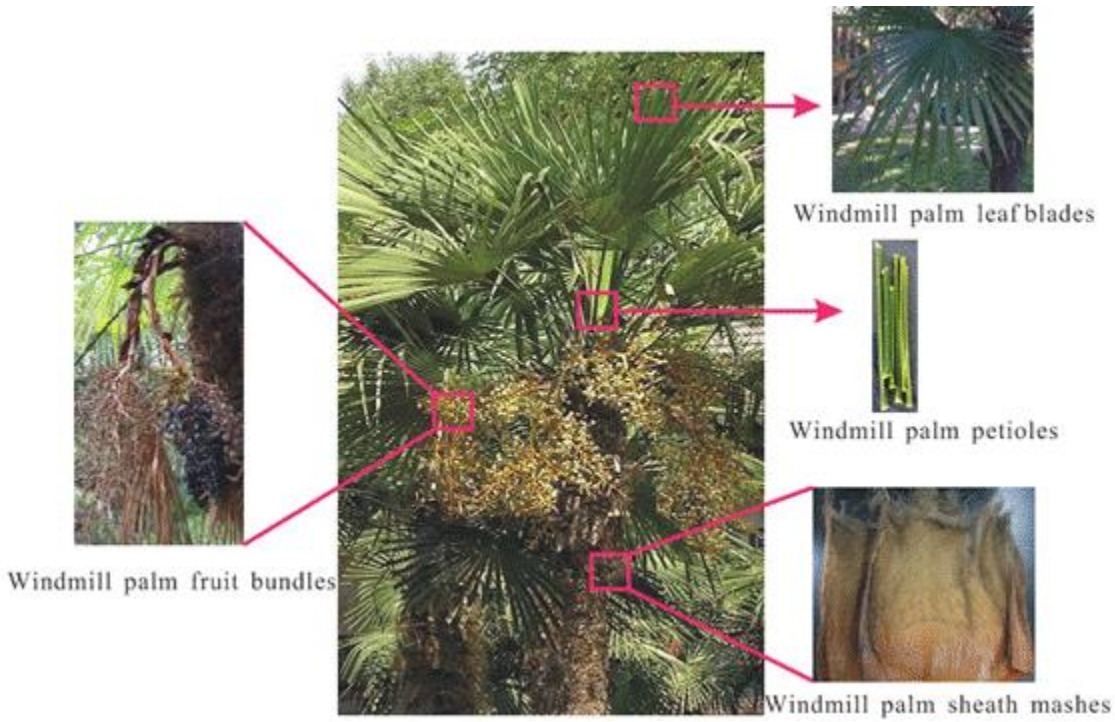

Fig. 1. Pictures of the raw materials from different morphological parts of windmill palm tree

The four kinds of raw materials were first treated with 4 wt.% hydrogen peroxide (H_2O_2) and 1.5 wt.% sodium hydroxide (NaOH) solutions with a 1:50 fiber-to-extractant ratio (g/mL) at 85 °C for 4 h. The residue of the windmill palm petiole fiber (PF), leaf blade fiber (LBF), leaf sheath fiber (LSF), and fruit bunch fiber (FBF) was washed with running water three times and then air-dried.

Methods

Chemical compositional analysis

Determination of the water solubility, solvent extractive properties, α-cellulose, and lignin contents were undertaken following the TAPPI standards: T207 cm-08 (2008), T204 cm-07 (2007), T203 cm-09 (2009), and T222 om-11 (2011). The ash content was measured from the difference between the initial weight of dried samples and that after calcination for 4 h at 800 °C. The holocellulose and hemicellulose contents were determined based on previous literature (Guimarães *et al.* 2009). Prior to determination of the chemical composition, all the windmill palm samples were oven-dried with air circulation at 60 °C for 24 h to eliminate moisture.

Scanning electron microscopic (SEM) evaluation

The surface morphology of the extracted fibers from different morphological parts of the windmill palm was examined using an SEM-EDX (TM3030, Hitachi, Tokyo, Japan) analyzer, which also provided the elemental compositions. The samples were fixed on aluminum stubs and then coated with gold by ion sputter (E-1045, Hitachi, Tokyo, Japan) to create a conductive surface. The accelerated voltage used was 5 kV.

Length, diameter, aspect ratio, and hollowness test

With the aid of an ultra-depth microscope (VHX-100, Keyence, Osaka, Japan), the length and diameter of the fibers extracted from various parts of the windmill palm tree were measured, and the aspect ratio (length/diameter) was then determined. The pictures of the cross-sections of these extracted fibers obtained *via* SEM were used to calculate the hollowness value. This was measured by considering the percentage difference between the area of the lumen in the middle of each fiber and the area of the whole fiber in the cross-section. For each type of fiber, 300 fibers were evaluated for their length, diameter, and hollowness values.

Fourier transform infrared (FTIR) spectroscopic analysis

The functional groups and the types of chemical bonding in windmill palm raw materials and fibers were determined using an FTIR spectrometer (Nicolet 5700, Nicolet, Madison, USA). The FTIR spectra of the pelletized samples were recorded in the frequency range of 500 cm^{-1} to 4000 cm^{-1}.

X-ray diffraction (XRD) analysis

The crystallinity of the fibers was determined using an X-ray powder diffractometer (Xpert-Pro MPD, Philips, Eindhoven, Holland). The samples were scanned over a 2θ range of 5° to 45°. The crystallinity index (CrI) was determined as stated by Segal *et al.* (1959), based on Eq. 1,

$$CrI\,(\%) = \frac{I_{002} - I_{am}}{I_{002}} * 100 \quad (1)$$

where I_{002} denotes the maximum intensity of the 002 peak at an approximate 2θ of 22° and I_{am} indicates the intensity of diffraction of the amorphous material, which was taken at an approximate 2θ of 18°.

Thermogravimetric analysis (TGA)

The TGA was performed using a TGA series thermo-gravimetric analyzer (5700, TA Instruments, New Castle, USA). The thermograms were acquired between 35 °C and 800 °C at a heating rate of 10 °C /min, with nitrogen as the purge gas at a flow rate of 50 mL/min.

RESULTS AND DISCUSSION

Chemical Compositions of Windmill Palm Materials

The chemical compositions of raw materials and the extracted fibers from different parts of the windmill palm tree are presented in Table 1. These results showed that the windmill palm was a lignocellulosic biomass with a low lignin content and high amount of α-cellulose.

The fractions P and LB had high levels of water-soluble materials, approximately 14%. The extractive content was highest in LB (8.65%) compared to the other materials. The high extractive and water-soluble contents were considered to play a negative role in paper production by reducing the pulp yield, and also may have a negative impact on chemical and mechanical pulping (Khalil *et al.* 2008).

A comparison of the mean values for α-cellulose, hemicellulose, and lignin contents of raw materials of windmill palm to other palm family fibers, such as oil palm (Hassan *et al.* 2010), sugar palm (Sahari *et al.* 2012), and other lignocellulosic materials (Oliveira *et al.* 2007) is shown in Table 1. The chemical compositions obtained in this study were similar to that of oil palm (Hassan *et al.* 2010). The LS material had the highest cellulose content (52.3%) among the four various types of raw materials from the windmill palm tree, whereas the cellulose contents for P, LB, and FB were nearly identical at approximately 40%. Cellulose is the main structural component with a strong effect on the mechanical properties, providing strength and stability to the plant cell walls and fibers (Sahari *et al.* 2012).

Generally, the fraction LB showed the highest percentage of lignin (26.4%), followed by fraction P (24.8%), LS (23.5%), and LB (16.6%). Lignin is a polymer that should be removed during pulping, but is also responsible for the toughness and stiffness properties (Khalil *et al.* 2008; Hassan *et al.* 2010) of the plants. The fraction LB had the lowest lignin content, which indicated that this material could undergo bleaching more easily.

The single fibers extracted from these raw materials had a higher cellulose content (more than 70%) and lower extractive and water-soluble contents (less than 2%) than the individual raw materials from windmill palm. Furthermore, also in comparison to other lignocellulosic materials, with the exception of bamboo (Zhang *et al.* 2015), the leaf sheath fiber (LSF) contained the highest percentage of holocellulose (89.5%) and α-cellulose contents (78.2%). In pulp and paper technology, the strength of paper depends on the content of cellulose in the plant source material (Khalil *et al.* 2008). This indicated that the LSF has the potential for better mechanical properties.

The elemental composition of ashes from windmill palm is shown in Table 2. Inorganic elements have a negative effect on the kraft pulping and paper qualities (Oliveira *et al.* 2007). The high ash content in windmill palm was considered as a disadvantage in the use of windmill palm as a raw material for pulp and paper production.

The elemental contents of chlorine, sulfur, and potassium were considerably reduced by treatment with a hot alkali solution, which indicated that the alkali treatment was sufficient for the removal of most of the impurities in raw materials, though the residual sodium concentration increased with the NaOH addition. A small amount of magnesium, silicon, calcium, and phosphorus remained in the ash of the fiber even after alkali treatment.

Table 1. Chemical Composition of Windmill Palm and Other Lignocellulosic Materials

Samples	Cold Water (%)	Hot Water (%)	Ben-ethanol (%)	Ash (%)	Lignin (%)	Holocellulose (%)	α-Cellulose (%)	Hemi-Cellulose (%)
P	13.97	3.38	2.28	4.69	24.83	68.44	39.49	28.96
LB	14.94	6.11	8.65	7.47	16.64	66.25	41.04	25.21
FB	5.75	3.35	4.68	4.06	26.37	60.07	38.02	22.05
LS	1.52	2.32	2.08	1.23	23.52	71.49	52.26	19.23
PF	1.07	1.02	1.03	3.87	8.13	85.42	76.97	8.45
LBF	0.87	0.73	0.67	6.40	6.38	83.23	71.48	11.75
FBF	0.92	0.80	0.85	1.96	6.93	86.49	77.06	9.43
LSF	0.85	0.78	0.69	0.54	7.24	89.50	78.18	11.32
Surgar Palm[a]	-	-	2.20～6.30	2.40～4.00	18.90～46.40	61.1～81.2	40.60～66.50	-
Oil Palm[b]	-	-	-	-	13.20～25.00	-	41.90～65.00	17.10～83.50
Banana[c]	3.80～15.10	-	0.90～2.60	11.60～26.80	9.70～18.00	20.3～62.7	14.40～39.50	5.50～21.50
Ramin[d]	-	-	-	-	0.60～0.70	-	67.76	13.00～16.00
Bamboo[d]	-	-	-	-	10.15	-	78.83	12.49
Coir[d]	-	-	-	-	38.00～45.00	-	32.00～53.00	0.15～15.00

Note: [a] from Sahari *et al.* (2012); [b] from Hassan *et al.* (2010); [c] from Oliveira *et al.* (2007); and [d] from Zhang *et al.* (2015)

Table 2. Elemental Composition of Ashes (%) from Windmill Palm

Samples	Carbon (%)	Oxygen (%)	Sodium (%)	Magnesium (%)	Silicon (%)	Chlorine (%)	Phosphorus (%)	Sulfur (%)	Potassium (%)	Calcium (%)
Raw Materials										
P	5.17	36.34	-	3.35	12.87	2.04	1.23	1.06	26.72	10.78
LB	3.12	39.14	-	2.00	21.99	6.47	2.28	1.23	9.73	12.87
FB	7.74	38.47	-	1.23	4.54	3.28	1.50	1.12	33.61	8.08
LS	2.23	54.61	-	4.29	10.46	1.12	1.04	3.62	5.96	15.07
Single Fibers										
PF	16.58	37.52	2.99	3.34	4.46	-	4.43	-	-	30.40
LBF	11.59	37.98	1.10	2.51	8.68	-	1.94	-	-	36.20
FBF	17.51	44.62	1.99	3.71	1.32	-	3.68	-	-	25.58
LSF	19.77	35.82	2.38	-	-	-	-	-	-	41.39

Morphological Properties of Raw Materials and extracted Fibers from Different Parts of Windmill Palm

The surface morphologies of raw materials and extracted fibers are shown in Fig. 2. Though the fractions P, LB, FB, and LS are four different types of materials from different morphological parts of windmill palm, they still possessed some similar characteristics. In the cross-sections, unlike the materials of most secondary xylem dicotyledons and gymnosperms, the raw materials of windmill palm are comprised of primary vascular bundles imbedded in parenchymatous ground tissues. This structure was observed in the longitudinal view of all of the four types of materials. Almost every bundle was made up of vessels, fibers, phloem, and parenchymatous tissues.

The vessels were formed by scalariform thickening of the lateral wall, which was characterized by the deposition of lignin and hemicelluloses (De Simas *et al.* 2010). These vessels were composed of dead cells, were substantially larger than any other cells, and mainly served to transport water and minerals to plant (Liu *et al.* 2005). The phloem observed in Fig. 2b was surrounded by sclerenchyma. Sclerenchyma consisted of cells with thickened walls, which were often lignified and were always categorized as fiber (De Simas *et al.* 2010). The cell walls of the fiber function in buckling resistance against lateral compression forces, providing elasticity and mechanical support to vascular bundles (Khalil *et al.* 2008). A few thick cell layers of fiber elements typically surround the vascular bundle in a monocot plant. For P, LB, and FB the thicknesses observed were 2 to 4, 4 to 6, and 4 to 8 layers, respectively. Fraction LS, as shown in Fig. 2d, had the thickest layers of fiber at more than 10 layers.

Single fibers extracted from the windmill revealed a slender shape with a tapering and sealing terminus without convolution. The windmill palm fiber had a honeycomb structure with thin walls and fairly wide cavities or spaces used to store water (Binoj *et al.* 2016) called lumens. The fraction FBF (Fig. 2c) had the largest diameter, which was nearly twice that of PF (Fig. 2a).

Morphometric Parameters of Windmill Palm Single Fibers

The length, diameter, aspect ratio, and hollowness of fibers extracted from various parts of windmill palm in comparison with other natural fibers are presented in Table 3. For fibers extracted from windmill palm, the fraction LBF was the largest with a length of approximately 1237.52±467.06 μm, followed by PF (1015.99±278.05 μm), FBF (919.47±252.25 μm), and LSF (637.96±182.20 μm). The fraction LSF exhibited the finest fiber diameter of approximately 10.02±1.78 μm, while the largest diameter was 20.56 ±5.63μm for the FBF fiber.

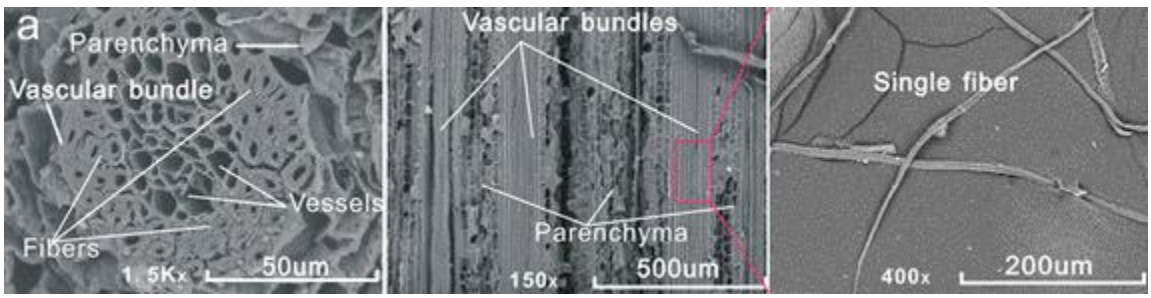

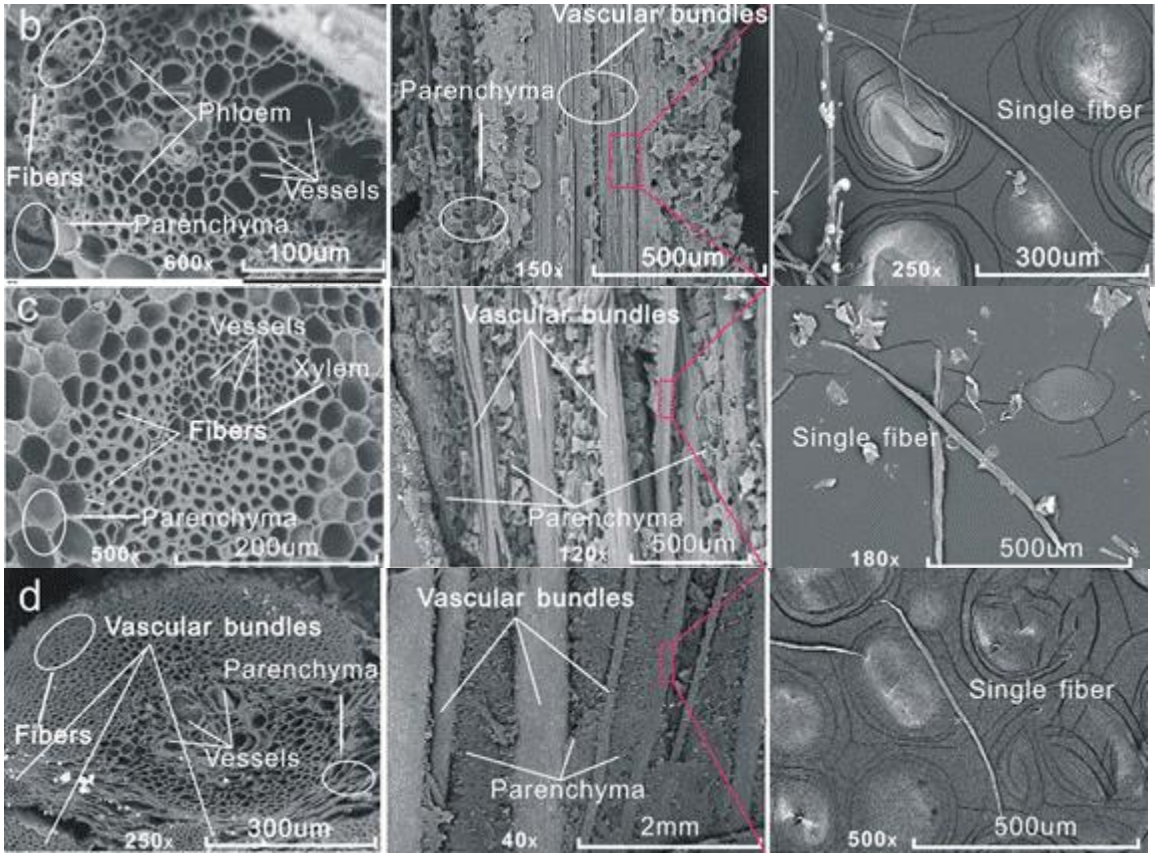

Fig. 2. Transverse sections and surface morphologies of raw materials and extracted fibers from various parts of windmill palm: a: windmill palm petiole (P), b: windmill palm leaf blade (LB), c: windmill palm fruit bunch (FB), and d: windmill palm leaf sheath (LS).

The aspect ratio of fiber had a marked effect on the mechanical properties, as well as on interfacial bonding for short fiber-reinforced composites (Nirmal *et al.* 2015). Among the four types of windmill palm single fibers, the LBF showed the highest aspect ratio, which resulted in enhanced mechanical properties compared to OPF (Hassan *et al*. 2010) and bamboo (Tokoro *et al.* 2008) fibers.

In addition to the aspect ratio, the proportion of cell wall is another important factor contributing to the fiber/matrix interface (Onyeagoro *et al.* 2012). The larger the hollowness of the fiber, the cell wall becomes thinner. As a result, the fiber with a high hollowness value had a low proportion of cell wall, which imparted a negative effect on the interfacial bonding. For short fiber-reinforced composites, the energy consumption was increased with increased fiber length during fiber pullout, thus it provided no fiber breakage (Tokoro *et al.* 2008). The LBF fraction had the longest length, highest aspect ratio, and lowest cell wall proportion. All these results indicated that LBF was the most suitable fraction to be used as a reinforcing fiber when compared with other windmill palm single fibers.

Table 3. Physical Parameters of extracted Fibers Obtained from Different Morphological Parts of Windmill Palm and Other Lignocellulosic Materials

Samples	Length (L)		Diameter (D)		Aspect Ratio (L/D)	Hollowness	
	(μm)	SE $\bar{x}$	(μm)	SE $\bar{x}$		(%)	SE $\bar{x}$
PF	1015.99	278.05	11.33	2.19	92.15	38.17	9.57
LBF	1237.52	467.06	10.62	3.86	121.39	38.27	9.22
FBF	919.47	252.25	20.56	5.63	46.99	53.84	10.01
LSF	637.96	182.20	10.02	1.78	65.50	47.21	11.10
Bamboo[a]	1220.00	-	18.80	-	65.00	-	-
OPF[a]	17500.00	-	151.50	-	115.50	-	-
Banana[b]	45000.00	-	150.00	-	300.00	-	-

Note: SE $\bar{x}$: Standard error of mean; and OPF: Oil palm fibers; [a] from Hassan *et al.* (2010); and [b] from Tokoro *et al.* (2008)

FTIR Structural Analysis

The changes in the chemical composition between the raw materials and the alkali-extracted single fibers were evaluated by FTIR spectroscopy. Figure 3 shows the spectra of raw materials, which indicated similar chemical compositions of extracted fibers.

In all of the samples, a large band at 3,300 cm^{-1} to 3,500 cm^{-1} related to the O-H stretching of hydrogen bonded hydroxyl (OH) groups of cellulose and absorbed water (Fahma *et al.* 2010) was observed. The peaks in the 2,900 cm^{-1} region were attributed to the aliphatic saturated C-H stretching vibration in cellulose, hemicellulose, and lignin components (Fahma *et al.* 2010).

It can be seen that the peak at 1720 cm^{-1} to 1733 cm^{-1} disappeared after the alkali treatment. This peak was assigned mainly to C=O stretching vibration of the carbonyl and acetyl groups in the xylan component of hemicellulose (Ibrahim *et al.* 2013). Other absorption bands of lignin at approximately 1610 cm^{-1} (Agblevor *et al.* 2007) disappeared in the extracted fibers. The peak formed at 1633 cm^{-1} to 1638 cm^{-1} confirmed the existence of celluloses. Moreover, the band near 1240 cm^{-1}, corresponded to the axial asymmetric stretching of =C-O-C of ether-, ester-, and phenolic groups (Ibrahim *et al.* 2013), appeared at a very low intensity in the extracted fibers in Fig. 3. The low intensity of this peak was due to the very low lignin and hemicellulose contents in the extracted fibers extracted by the alkali treatment. This also demonstrated the almost complete removal of lignin and hemicelluloses by the chemical treatment.

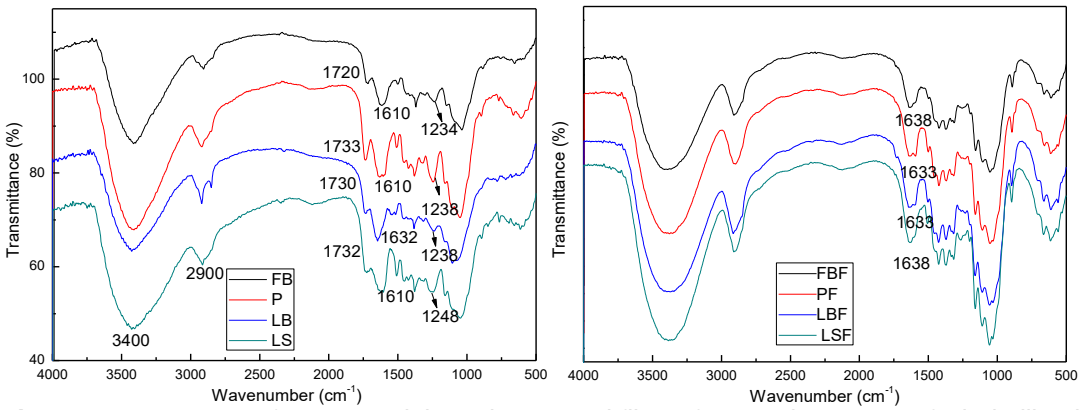

Fig. 3. FT-IR spectra of raw materials and extracted fibers from various parts of windmill palm

X-ray Diffraction and Crystallinity Measurements

The XRD studies were conducted to evaluate the crystalline properties of raw materials and alkali-treated fibers from windmill palm. Celluloses are semicrystalline biopolymers known to possess both crystalline and amorphous domains in their molecular structure (Goh *et al.* 2016). As shown in Fig. 4, the typical X-ray diffractograms obtained for all of the powdered windmill palm raw materials and extracted fiber samples exhibited the typical semi-crystalline patterns with an amorphous broad hump and a crystalline peak (Goh *et al.* 2016). All of the samples possessed diffraction peaks centered at approximately 16° (overlapping of the characteristic 101 and 10ī planes), 22° (correspond to 002 plane), and 34° (correspond to 040 plane), which are characteristics of cellulose-I (Ortunati *et al.* 2013).

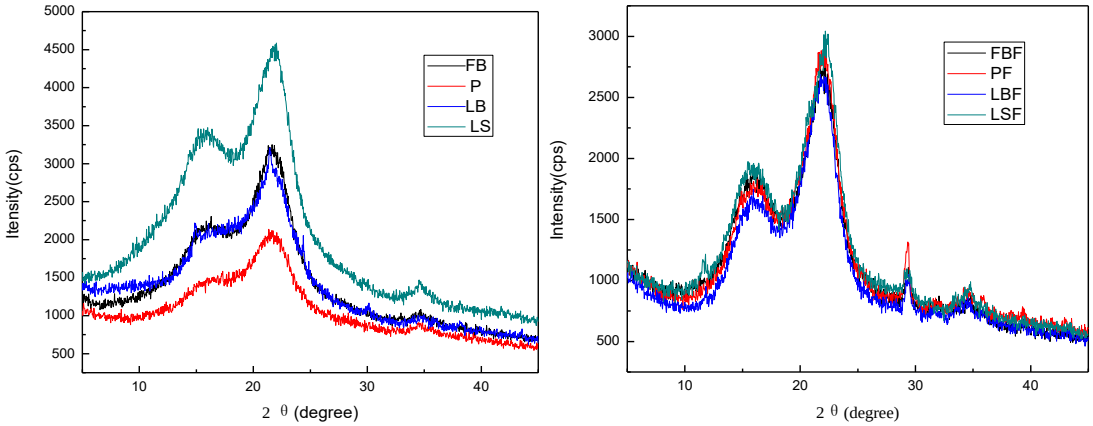

Fig. 4. X-ray diffractograms for raw materials and single fibers from various parts of windmill palm

The crystallinity index (CrI) is frequently used to describe the ordered structure and the relative amount of crystalline material present in cellulose (Ortunati *et al*. 2013). The results obtained from the XRD analyses are presented in Table 4. The CrI of fractions P, LB, FB, and LS were calculated as 31%, 31%, 26%, and 34%, respectively. The lowest crystallinity index was found with the sample of FB, which corresponded to its lowest cellulosic content (38.02%) in the sample (Chaker *et al.* 2014). The CrI for PF, LBF, FBF, and LSF fractions were 46%, 44%, 46%, and 49%, respectively. The increased crystallinity observed after the alkali treatment was related to the increased rigidity and stiffness properties of the cellulose structure, which led to a higher tensile strength and Young's modulus of the fibers (Haafiz *et al.* 2013; Goh *et al.* 2016).

After the alkali treatment, the crystallinity indices were anticipated to be higher than those for the raw materials because of the partial hemicelluloses and lignin removal, which were considered to have no contributions to the crystallinity (Goh *et al*. 2016). However, cellulose has a portion of imperfect crystallites that also contribute to the amorphous content of the lignocellulosic biomass (Mendes *et al*. 2015). As a result, the CrI of all of the samples was lower than the cellulose content (Table 1).

Table 4. Crystalline Parameters Obtained from XRD of Samples from Windmill Palm

Samples	Peak Position (2θ)	I_{002} (cps)	Peak Position (2θ)	I_{am} (cps)	CrI (%)
Raw Materials					
P	21.78	4471	18.31	3086	31
LB	21.69	1853	17.81	1286	31
FB	21.53	2905	17.89	2138	26
LS	21.61	3148	18.10	2093	34
Extracted Fibers					
PF	22.02	2629	18.20	1410	46
LBF	22.11	2684	18.36	1500	44
FBF	21.93	2788	18.30	1504	46
LSF	22.26	2966	18.14	1521	49

Note: I_{002} denotes the maximum intensity of the 002 peak at an approximate 2θ of 22° and I_{am} indicates the intensity of diffraction of the amorphous material at an approximate 2θ of 18°

Thermal Properties

Typical weight loss *versus* temperature plots for the raw materials and alkali-treated fibers are presented in Fig. 5. The main peaks observed in the TGA were characterized by two-step degradations over the range of temperatures tested. An initial weight loss was observed between 50 °C and 150 °C for almost all of the samples, due to the loss of moisture content and low volatile compounds (Chowdhury *et al*. 2013). The next sharp degradation began at elevated temperatures and corresponded to the degradation of hemicellulose, cellulose, lignin, *etc*. (Chowdhury *et al*. 2013).

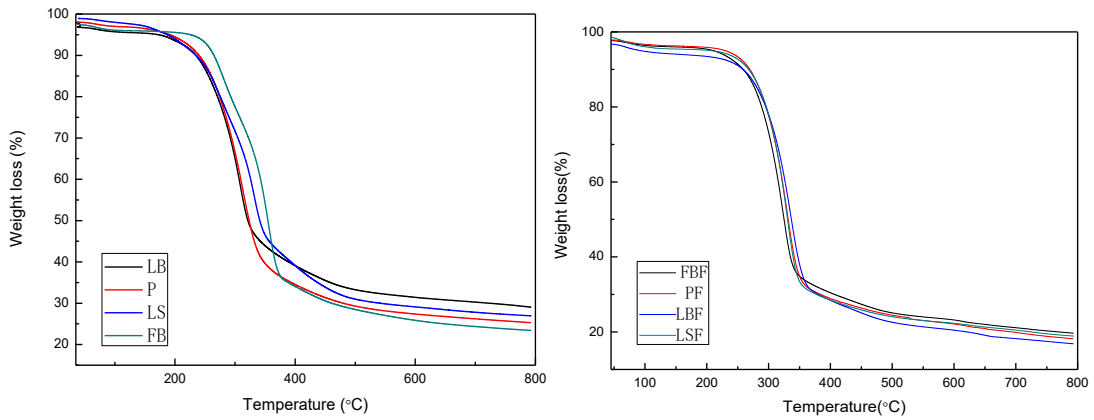

Fig. 5. TGA curves of the materials

The derivative thermo-gravimetric (DTG) curves were generated from the differentiation of TGA curves (weight by percentage, wt.%), which provided information about the temperature at which the weight loss was most dramatic. The results are illustrated in Table 5 (Mohtar *et al.* 2015).

Almost all of the extracted fibers extracted by the alkali treatment showed a higher onset temperature than the raw materials. The thermal depolymerization of hemicellulose and the cleavage of the glycosidic linkages of cellulose polymers occurred at a low temperature region ranging from 220 °C to 300 °C (Costa *et al*. 2013). The complete degradation of cellulose took place between 275 °C and 400 °C (Deepa *et al.* 2011; Costa *et al.* 2013). The increase in the onset temperature corresponded to the removal of hemicellulose, which could occur at a low temperature, before the degradation of cellulose (Mohtar *et al*. 2015). However, the LS had the highest onset temperature of approximately 319 °C potentially due to the presence of silica bodies on the surface.

Table 5. Degradation Characteristics and the Percentage Residue Left from the Raw Materials and Extracted Fibers

Materials	Onset Degradation (°C)	Main Degradation Step (°C)	Residue after Heating at 450 °C (%)
Raw Materials			
FB	290	317	35.50
P	292	322	31.37
LB	304	338	33.89
LS	319	366	30.57
Extracted Fibers			
FBF	303	327	27.39
PF	310	338	26.36
LBF	312	340	25.09
LSF	311	338	25.87

CONCLUSIONS

1. Eight samples (raw materials and extracted fibers) isolated from four different morphological parts of windmill palm were characterized. Among the four types of raw materials tested, the LS fraction had the highest cellulose content of 52.3%, making it the most efficient fraction for fiber extractions. Among the extracted fibers LSF contained the highest percentage of holocellulose of 89.5%.
2. The raw materials of windmill palm consisted of primary vascular bundles imbedded in parenchymatous ground tissues. Single fibers extracted from the windmill palm showed a slender shape with a tapering and sealing terminus, and a lumen in the cross-section. The LBF had the longest length (1240 μm ± 467 μm), highest aspect ratio (121.4), and lowest cell wall proportion, giving the LBF fraction great potential as a reinforced fiber.
3. The extracted fibers are almost free from lignin and hemicellulose. As a result, an increase in the crystallinity of extracted fibers (above 44%) was observed, while the

CrI for raw materials was below 35%. The fraction LS possessed the highest onset temperature and main degradation temperature of 319 °C and 366 °C, respectively.

ACKNOWLEDGMENTS

This work was funded by the Priority Academic Program Development of Jiangsu Higher Education Institutions, China (No. 37 2014), and the Jiangsu Province Special Project, China (No. BY2014083).

REFERENCES CITED

Agblevor, F. A., Ibrahim, M. M., and El-Zawawy, W. K. (2007). "Coupled acid and enzyme mediated production of microcrystalline cellulose from corn cob and cotton gin waste," *Cellulose* 14(3), 247-256. DOI: 10.1007/s10570-006-9103-y

Binoj, J. S., Raj, R. E., Sreenivasan, V. S., and Thusnavis, G. R. (2016). "Morphological, physical, mechanical, chemical, and thermal characterization of sustainable Indian *Areca* fruit husk fibers (*Areca catechu L.*) as potential alternate for hazardous synthetic fibers," *Journal of Bionic Engineering* 13(1), 156-165. DOI: 10.1016/S1672-6529(14)60170-0

Chaker, A., Mutje, P., Vilar, M. R., and Boufi, S. (2014). "Agriculture crop residues as a source for the production of nanofibrillated cellulose with low energy demand," *Cellulose* 21(6), 4247-4259. DOI: 10.1007/s10570-014-0454-5

Chowdhury, N. K., Beg, M. D. H., Khan, M. R., and Mina, M. F. (2013). "Modification of oil palm empty fruit bunch fibers by nanoparticle impregnation and alkali treatment," *Cellulose* 20(3), 1477-1490. DOI: 10.1007/s10570-013-9921-7

Costa, L. M. M., De-Olyveira, G. M., Cherian, B. M., Leao, A. L., De-Souza, S. F., and Ferreira, M. (2013). "Bionanocomposites from electrospun PVA/pineapple nanofibers/*Stryphnodendron adstringens* bark extract for medical applications," *Industrial Crops and Products* 41, 198-202. DOI: 10.1016/j.indcrop.2012.04.025

Deepa, B., Abraham, E., Cherian, B. M., Bismarc, A., Blaker, J. J., Pothan, L. A., Leao, A. L., Souza, S. F., and Kottaisamy, M. (2011). "Structure, morphology, and thermal characteristics of banana nano fibers obtained by steam explosion," *Bioresource Technology* 102(2), 1988-1997. DOI: 10.1016/j.biortech.2010.09.030

De Simas, K. N., Vieira, L. d. N., Podesta, R., Vieira, M. A., Rockenbach, I. I., Petkowicz, C. L., de Deus Medeiros, J., de Francisco, A., Amante, E. R., and Amboni, R. D. (2010). "Microstructure, nutrient composition and antioxidant capacity of king palm flour: A new potential source of dietary fiber," *Bioresource Technology* 101(14), 5701-5707. DOI: 10.1016/j.biortech.2010.02.053

Fahma, F., Iwamoto, S., Hori, N., Iwata, T., and Takemura, A., (2010). "Isolation, preparation, and characterization of nanofibers from oil palm empty-fruit-bunch (OPEFB)," *Cellulose* 17(5), 977-985. DOI: 10.1007/s10570-010-9436-4

Goh, K. Y., Ching, Y. C., Chuah, C. H., Abdullah, L. C., and Liou, N. S. (2016). "Individualization of microfibrillated celluloses from oil palm empty fruit bunch: Comparative studies between acid hydrolysis and ammonium persulfate oxidation," *Cellulose* 23(1), 379-390. DOI: 10.1007/s10570-015-0812-y

Guimarães, J. L., Frollini, E., da Silva, C. G., Wypych, F., and Satyanarayana, K. G. (2009). "Characterization of banana, sugarcane bagasse, and sponge gourd fibers of Brazil," *Industrial Crops and Products* 30(3), 407-415. DOI: 10.1016/j.indcrop.2009.07.013

Haafiz, M. K. M., Hassan, A., Zakaria, Z., Inuwa, I. M., and Islam, M. S. (2013). "Physicochemical characterization of cellulose nanowhiskers extracted from oil palm biomass microcrystalline cellulose," *Materials Letters* 113, 87-89. DOI: 10.1016/j.matlet.2013.09.018

Hassan, A., Salema, A. A., Ani, F. N., and Abu Baker, A. (2010). "A review on oil palm empty fruit bunch fiber-reinforced polymer composite materials," *Polymer Composites* 31(12), 2079-2101. DOI: 10.1002/pc.21006

Ibrahim, M. M., El-Zawawy, W. K., Juettke, Y., Koschella, A., and Heinze, T. (2013). "Cellulose and microcrystalline cellulose from rice straw and banana plant waste: Preparation and characterization," *Cellulose* 20(5), 2403-2416. DOI: 10.1007/s10570-013-9992-5

Ishak, M. R., Sapuan, S. M., Leman, Z., Rahman, M. Z. A., Anwar, U. M. K., and Siregar, J. P. (2013). "Sugar palm (*Arenga pinnata*): Its fibres, polymers, and composites," *Carbohydrate Polymers* 91(2), 699-710. DOI: 10.1016/j.carbpol.2012.07.073

Jammy. R., Japar, S., and Shah, M. K. M. (2015). "Physicochemical and mechanical properties of different morphological parts of the Tea Tree (*Melaleuca alternifolia*) fibres," *Fibres & Textiles in Eastern Europe* 23, 31-36. DOI: 10.5604/12303666.1167414

Khalil, H. A., Bhat, I. U. H., Jawaid, M., Zaidon, A., Hermawan, D., and Hadi, Y. S. (2012). "Bamboo fibre reinforced biocomposites: A review," *Materials & Design* 42, 353-368.

Khalil, H. A., Tye, Y. Y., Chow, S. T., Saurabh, C. K.,Paridah, M. T., Dungani, R., and Syakir, M. I. (2016). "Cellulosic pulp fiber as reinforcement materials in seaweed-based film," *BioResources* 12(1), 29-42.

Khalil, H. P. S. A., Alwani, M. S., Ridzuan, R., Kamarudin, H., and Khairul, A. (2008). "Chemical composition, morphological characteristics, and cell wall structure of Malaysian oil palm fibers," *Technology and Engineering* 47(3), 273-280. DOI: 10.1080/03602550701866840

Liu, R. G., Yu, H., and Huang, Y., (2005). "Structure and morphology of cellulose in wheat straw," *Cellulose* 12(1), 25-34. DOI: 10.1007/s10570-004-0955-8

Liu, L., Wang, Q., Cheng, L., Qian, J., and Yu, J. (2011). "Modification of natural bamboo fibers for textile applications," *Fibers and Polymers* 12(1), 95-103. DOI: 10.1007/s12221-011-0095-3

Mendes, C. A. C., Adnet, F. A. O., Leite, M. C. A. M., Furtado, C. R. G., and Sousa, A. M. F. (2015). "Chemical, physical, mechanical, thermal and morphological characterization of corn husk residue," *Cellulose Chemistry and Technology* 49(9-10), 727-735.

Mohtar, S. S., Busu, T., Noor, A. M. M., Shaari, N., Yusoff, N. A., Khalil, M. A. B., Mutalib, M. I. A., and Mat, H. B. (2015). "Extraction and characterization of lignin from oil palm biomass *via* ionic liquid dissolution and non-toxic aluminum potassium sulfate dodecahydrate precipitation processes," *Bioresource Technology* 192, 212-218. DOI: 10.1016/j.biortech.2015.05.029

Nirmal, U., Hashim, J., and Ahmad, M. M. H. M. (2015). "A review on tribological performance of natural fibre polymeric composites," *Tribology International* 83, 77-104. DOI: 10.1016/j.triboint.2014.11.003

Oliveira, L., Cordeiro, N., Evtuguin, D. V., Torres, I. C., and Silvestre, A. J. D. (2007). "Chemical composition of different morphological parts from 'Dwarf Cavendish' banana plant and their potential as a non-wood renewable source of natural products," *Industrial Crops and Products* 26(2), 163-172. DOI: 10.1016/j.indcrop.2007.03.002

Onyeagoro, G. N. (2012). "Influence of surface lignin concentration on fiber surface characteristics and tensile properties of oil palm fiber/urea-formaldehyde resin composite," *Academic Research International* 3(1), 491.

Ortunati, E., Puglia, D., Monti, M., Santulli, C., Maniruzzaman, M., Foresti, M. L., Vazquez, A., and Kenny, J. M. (2013). "Okra (*Abelmoschus esculentus*) fibre based PLA composites: Mechanical behaviour and biodegradation," *Journal of Polymers and the Environment* 21(3), 726-737. DOI: 10.1007/s10924-013-0571-5

Sahari, J., Sapuan, S. M., Ismarrubie, Z. N., and Rahman, M. Z. A. (2012). "Physical and chemical properties of different morphological parts of sugar palm fibres," *Fibres & Textiles in Eastern Europe* 20, 21-24.

Sreekala, M. S., George, J., Kumaran, M. G., and Thomas, S. (2002). "The mechanical performance of hybrid phenol-formaldehyde-based composites reinforced with glass and oil palm fibres," *Composites Science and Technology* 62(3), 339-353. DOI: 10.1016/S0266-3538(01)00219-6

T207 cm-08 (2008). "Water solubility of wood and pulp," TAPPI Press, Atlanta, Georgia.

T204 cm-07 (2007). "Solvent extractives of wood and pulp," TAPPI Press, Atlanta, Georgia.

T203 cm-09 (2009). "Alpha-, beta-, and gamma-cellulose in pulp," TAPPI Press, Atlanta, Georgia.

T222 om-11 (2011). "Acid-insoluble lignin in wood and pulp," TAPPI Press, Atlanta, Georgia.

Tokoro, R., Vu, D. M., Okubo, K., Tanaka, T., Fujii, T., and Fujiura, T. (2008). "How to improve mechanical properties of polylactic acid with bamboo fibers," *Journal of Materials Science* 43(2), 775-787. DOI: 10.1007/s10853-007-1994-y

Wang, X., Hu, J., Liang, Y., and Zeng, J. (2011). "TCF bleaching character of soda-anthraquinone pulp from oil palm frond," *BioResources* 7(1), 0275-0282.

Xiang, H. F., Wang, D., Liu, H. C., Zhao, N., and Xu, J. (2013). "Investigation on sound absorption properties of kapok fibers," *Chinese Journal of Polymer Science* 31(3), 521-529. DOI: 10.1007/s10118-013-1241-8

Yang, X., Liu, X., Shang, L., Ma, J., Tian, G., and Yang, S. (2015). "Variation of tensile properties of single fibres of *Dendrocalamus farinosus* bamboo," *BioResources* 11(1), 1609-1619. DOI: 10.15376/biores.11.1.1609-1619

Yunos, N. S. H. M., Baharuddin, A. S., Yunos, K. F. M., Hafid, H. S., Busu, Z., Mokhtar, M. N., and Som, A. M. (2014). "The physicochemical characteristics of residual oil and fibers from oil palm empty fruit bunches," *BioResources* 10(1), 14-29. DOI: 10.15376/biores.10.1.14-29

Zhai, S. C., Li, D. G., Pan, B., Sugiyama, J., and Itoh, T. (2012). "Tensile strength of windmill palm (*Trachycarpus fortunei*) fiber bundles and its structural implications," *Journal of Materials Science* 47(2), 949-959. DOI: 10.1007/s10853-011-5874-0

Zhang, T., Guo, M., Cheng, L., and Li, X. (2015). "Investigations on the structure and properties of palm leaf sheath fiber," *Cellulose* 22(2), 1039-1051. DOI: 10.1007/s10570-015-0570-x

Article submitted: December 18, 2016; Peer review completed: March 3, 2017; Revised version received: March 18, 2017; Accepted: March 19, 2017; Published: March 27, 2017.
DOI: 10.15376/biores.12.2.3504-3520